A CORRELATIVE TECHNIQUE FOR CORRECTION OF SHADING EFFECTS IN DIGITAL MULTISPECTRAL VIDEO IMAGERY.

Cindy Ong

CSIRO, The Leeuwin Centre for Earth Sensing Technologies
Private Bag, P.O. Wembley, W.A. 6014. Tel: (09) 387 0243 Fax: (09) 387 0121

KEY WORDS: Method, Correlation, Correction, Multispectral, Video

ABSTRACT

This paper describes a technique for the removal of shading effects, caused by solar geometry and shadows, from airborne Digital Multi-Spectral Videography (DMSV) images acquired over the Comalco bauxite mines in North Queensland, Australia. The approach involves use of near-simultaneously acquired Landsat Thematic Mapper (TM) satellite data. The correlative technique produces imagery that retains a stable dynamic range and has very high numerical coherence in the overlap areas of sequential images. Calibration of the images to reflectances, using field spectral data, is performed before production of the seamless mosaics. The results of classification, using the corrected dataset, confirmed the adequacy of the correction procedure for its intended use in minesite rehabilitation monitoring. This paper describes the development and implementation of the technique and gives examples of the correction.

Introduction

Shading effects across Digital Multi-Spectral Video (DMSV) images (Lyon et al., 1994), sometimes called the "hot-spot" effect, is a significant problem. It is often referred to as the bi-directional reflectance factor, cross-scene or cross-track brightness, or differential illumination. It is visible on most aerial photographs and video images, appearing at the point on the ground in line with the aircraft and the sun. (The sun is in effect eclipsed by the aircraft). Maximum image-brightness surrounds that point as there is no visible shadow from vegetation structure. As the radial distance increases, so also does the amount of visible shadow in the image, causing reduced total reflectance. The shading is also dependant on particles in the atmosphere, pathlength, wavelength and the nature of the component surface material. Figure 1 shows an example of shading across two DMSV frames.

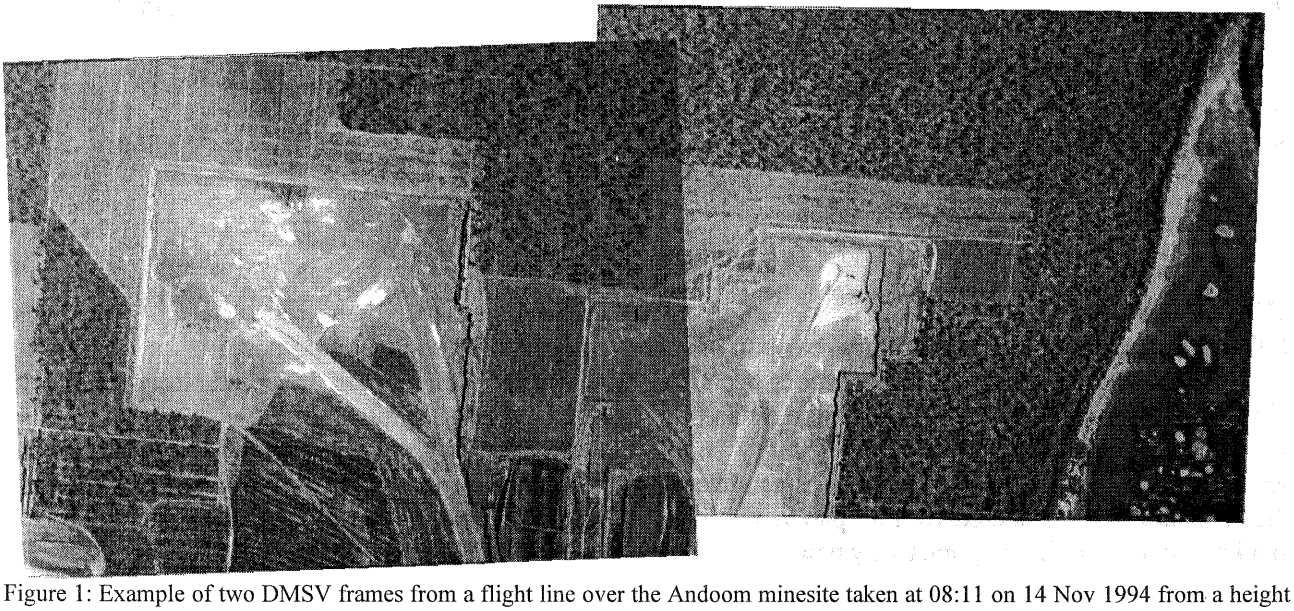

Figure 1: Example of two DMSV frames from a flight line over the Andoom minesite taken at 08:11 on 14 Nov 1994 from a height of 10,000 feet with a maximum 37° field of view.

Methods for removing shading by calculating a surface of average brightness, from a sequence of "uniform" frames in the flight line, and subtracting that surface from each image were evaluated. However, with the Weipa data, we were unable to obtain a satisfactory result. Most of the DMSV images covering the Weipa and Andoom minesites contain highly variable land cover, making it impossible to obtain enough uniform frames to derive an appropriate correction.

In his analysis of video data, King (1991) showed that, where the linear trends were consistent in all bands, simple band-ratios were a very effective means of reducing differential illumination caused by view angle. This method was also tried with unsatisfactory results. Rayleigh scattering effects vary for each waveband, being greater in the shorter wavelength bands. Such effects, prominent in the Comalco data, seem to contradict King's assumptions.

Pickup et al. (1995) indicated that a single equation, based on view angle, can be used for scene-brightness normalisation. Their findings show that this produces results better than the commonly used band-ratio techniques. This method was tried with data collected at another minesite but to date the results have not been thoroughly analysed.

The mining industry is vital to the Australian economy, but mining activity inevitably causes environmental impacts. Usually the miner must rehabilitate areas of disturbance to a condition satisfactory to the relevant government legislation. In Comalco's bauxite mines at Weipa and Andoom, North Queensland, Australia, DMSV data were collected by SpecTerra Systems (STS) in November, 1994. This system was chosen because it gives a non-invasive, high-resolution, timely and cost-effective method of quantitatively monitoring a large-scale rehabilitation operations.

A total of 196 frames of DMSV data, each being approximately 1x1.5 kilometre. with 2 metre spatial resolution, were collected over the Weipa and Andoom minesites on the 12th, 13th and 14th of November, 1994. The objective was to produce digital and photographic mosaics for quantitative measurement of the vegetation status. Before this could be achieved, it was necessary to remove 'artefacts' inherent in the DMSV data, of which shading is the most significant.

For this work spaceborne data, acquired at about the same time (10th November, 1994) as the DMSV image, were used as uniformly illuminated 'flat' image to derive a shading surface for correcting the DMSV data. Landsat TM bands 1, 2, 3, and 4 have band-centres close to the band-centres of the DMSV (Table 1). The correction method exploits this similarity by correlating the DMSV data with the near-simultaneously acquired TM imagery. The wavebands of the field radiometer, used for the calibration of the DMSV images, are also included in Table 1.

Methods

Table 1: Wavelengths of Landsat TM, DMSV and Exotech Radiometer bands

sensor	band 1	band 2	band 3	band 4
Landsat TM	450 - 520 (nm)	520 - 600 (nm)	600 - 690 (nm)	760 - 900 (nm)
DMSV	438 - 462 (nm)	538 - 562 (nm)	638 - 762 (nm)	758 - 782 (nm)
Exotech	450 - 480 (nm)	500 - 600 (nm)	600 - 700 (nm)	700 - 800 (nm)

All solar-illuminated remotely sensed data exhibit some amount of differential shading. However, it is assumed for this correction method, that the shading variation is insignificant in the portion of the Landsat TM image used for correcting the DMSV dataset. Figure 2 illustrates a hypothetical illumination curve across a Landsat TM image. Although this differential shading would be significant were the whole of this image used in the analysis, for a small portion of it the shading can be assumed negligible. Figure 3 compares the Landsat TM subset used with a DMSV frame. As illustrated, the area used for the correction is small and the shading is negligible therefore the shading curve across this subset is assumed to be "flat".

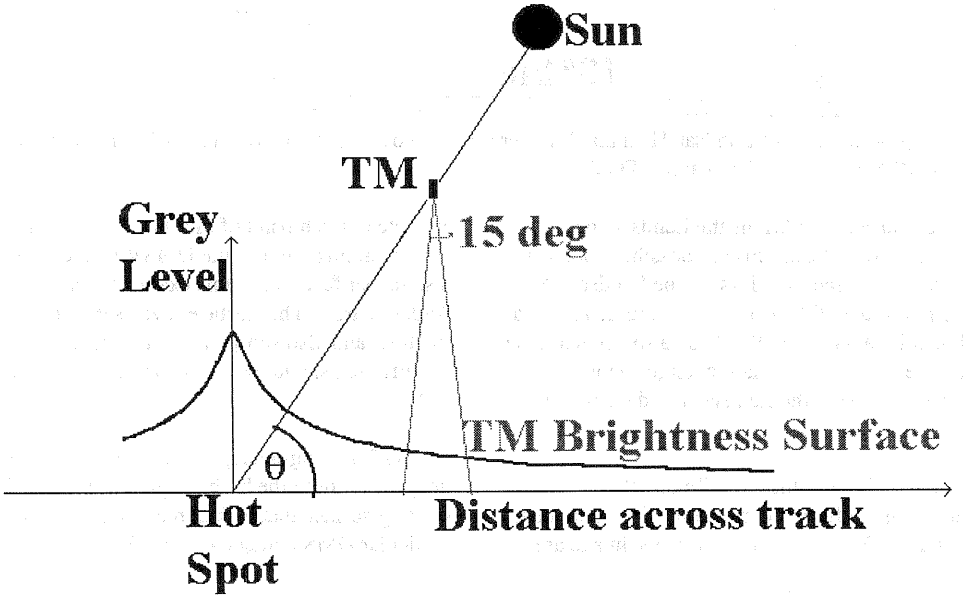

Figure 2. Shading across a Landsat TM frame, for a given sun elevation angle θ°.

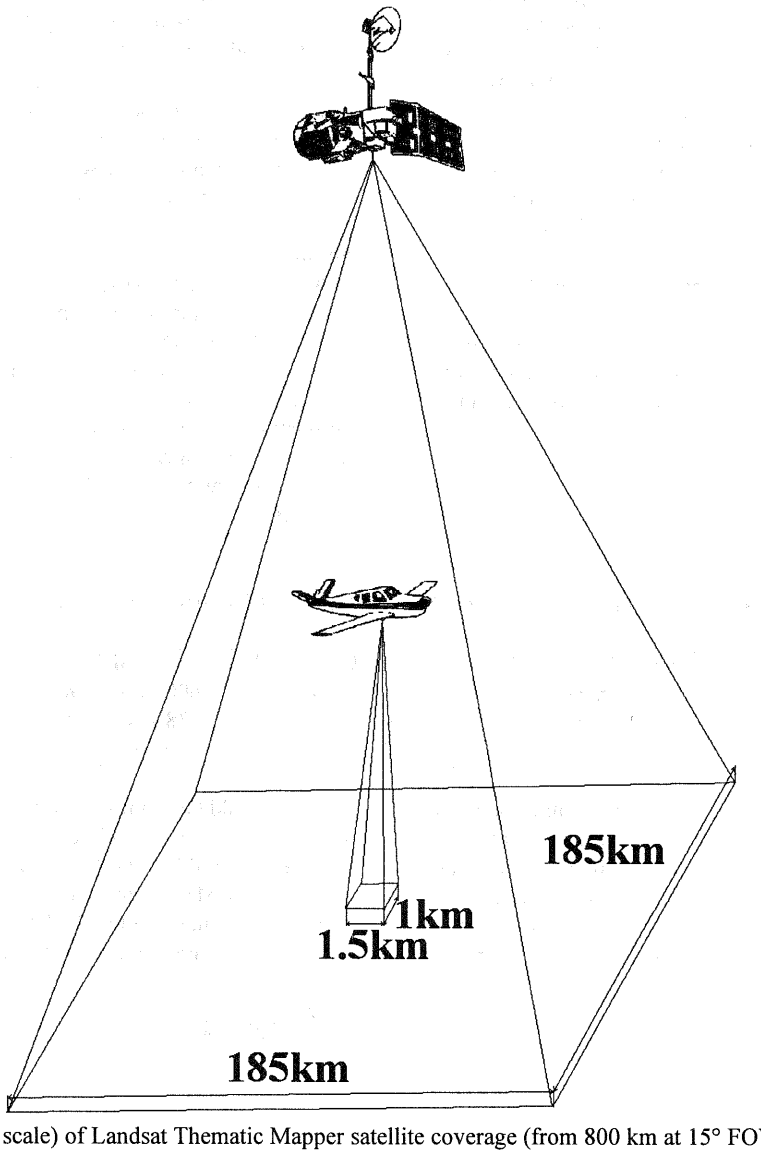

Figure 3: A diagram (not to scale) of Landsat Thematic Mapper satellite coverage (from 800 km at 15° FOV) in one scene compared with one frame of DMSV data (from 3 km at 37° FOV).

To preclude changed surface conditions the Landsat and DMSV data acquisition times should be as close as possible. Some TM processing must precede correction. Firstly, the Landsat TM image is co-registered to the DMSV mosaic. Landsat TM data have a smaller dynamic range than DMSV data so needed to be scaled to approximately the same dynamic range. This is achieved by linearly regressing the Landsat TM data on the DMSV data.

Each DMSV image has slightly different, illumination characteristics requiring a different correction. The coincident portions of the Landsat TM image and the DMSV image are extracted. Each band of this TM subset is subtracted from the corresponding band of the DMSV image. Figure 4 is the residual surface for, in this example a band 3 image from the Andoom area. This surface reveals differences relating to shading, and also shows as high frequency noise, the effects of the different spatial resolutions (2 m for DMSV versus 30 m for TM).

A 25x25 moving-average filter was applied to each residual image to smooth the high-frequency effects. This reveals the shading surface that is then removed from that band of that particular DMSV image (Figure 5).

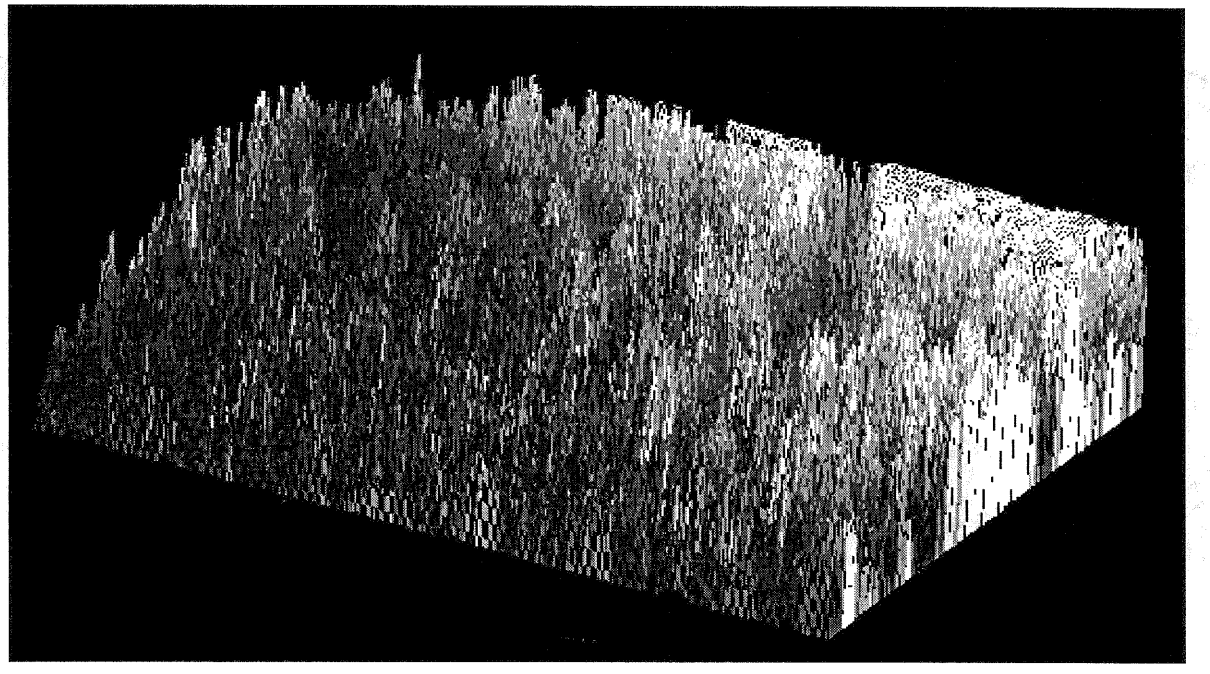

Figure 4. A 3-D example of the band 3 residual surface before smoothing.

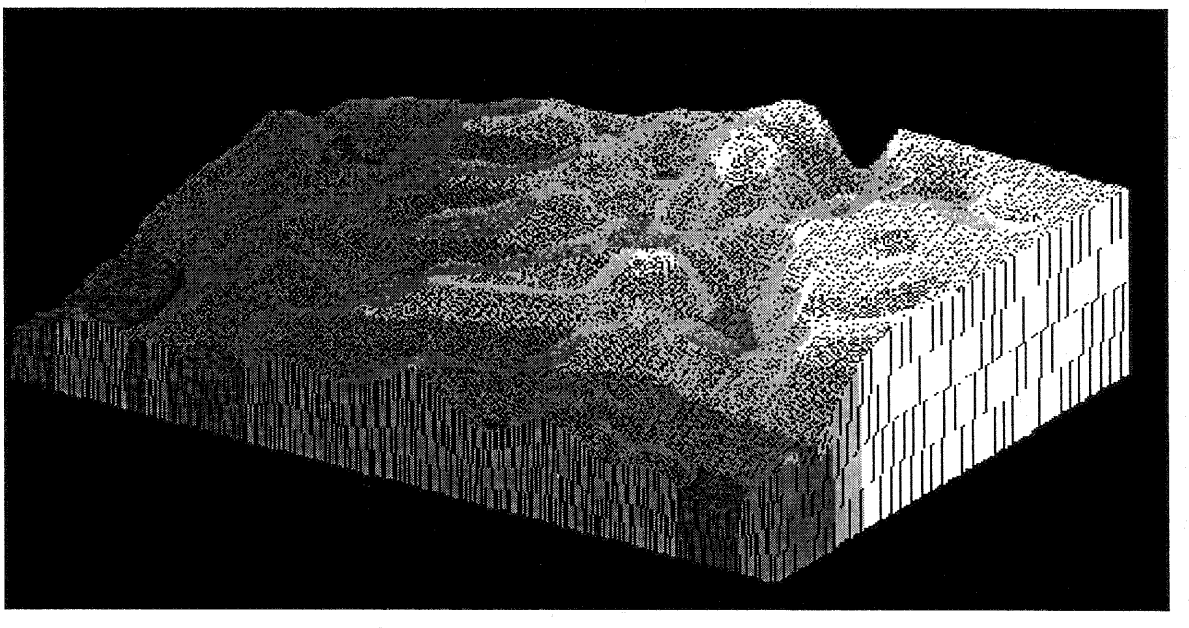

Figure 5. An example of the shading surface extracted from a band 3 DMSV image after the 25x25 smoothing.

Results

Following this procedure, the 196 differently illuminated DMSV images covering the minesites of Andoom and Weipa could be seamlessly mosaicked. The data over these two minesites were collected on separate occasions with different camera settings. Figure 6 shows, after correction, the same two frames as Figure 1.

Figure 6. Examples of two frames of corrected DMSV data.

To determine the validity of the correction, common areas from overlapping images, were extracted and the means and standard deviation statistics were compiled. Table 2 is an example of four common areas that had different illumination in the raw data and Table 3 shows similar areas after the correction.

Table 2. The means, standard deviation and area summary of four common areas extracted from overlapping areas before the correction procedure.

Comparison of Means in overlap area of raw images 2b and 2c								
	2b band1	2c band1	2b band2	2c band2	2b band3	2c band3	2b band4	2c band4
Minefloor	65	51.8	37.6	23.3	32.6	19.7	99.7	80.3
Regen 1	33.9	27.3	35.6	23.4	30.2	18.2	69.9	75.1
Native	25.3	19.5	29.0	18.7	22.0	12.2	70.9	59.0
Regen 2	30.9	26.2	34.9	24.2	30.4	19.8	56.0	44.5

Comparison of Standard Deviations in overlap area of raw images 2b and 2c								
	2b band1	2c band1	2b band2	2c band2	2b band3	2c band3	2b band4	2c band4
Minefloor	3.9	3.3	3.4	2.8	3.0	2.4	5.2	4.9
Regen 1	5.4	5.0	4.1	4.2	3.9	3.6	6.9	7.7
Native	5.1	4.4	6.9	5.5	4.1	3.6	15.4	14.2
Regen 2	4.7	3.9	5.6	5.4	4.5	4.6	7.5	5.9

Area Summary (number of pixels)		
	Frame 2b	Frame 2c
Mine floor	5233	5224
Regeneration 1	1626	1660
Native vegetation	6443	6511
Regeneration 2	1428	1447

Table 3 The means, standard deviation and area summary of the four common areas extracted from the overlapping areas after the correction procedure.

Comparison of Means in overlap area of corrected images 2b and 2c								
	2b band1	2c band1	2b band2	2c band2	2b band3	2c band3	2b band4	2c band4
Minefloor	45.2	45.1	51.5	51.5	52.6	52.5	97.2	97.1
Regen 1	38.3	38.3	39.3	40.2	36.1	36.8	75.1	75.6
Native	25.3	25.3	33.6	33.7	32.0	32.1	83.0	83.1
Regen 2	46.6	46.9	40.5	40.5	36.8	36.8	64.6	64.7

Comparison of Standard Deviations in overlap area of corrected images 2b and 2c								
	2b band1	2c band1	2b band2	2c band2	2b band3	2c band3	2b band4	2c band4
Minefloor	3.7	3.5	2.9	2.7	2.4	1.9	4.6	4.5
Regen 1	5.0	4.7	3.6	3.7	3.4	3.3	7.7	7.1
Native	5.3	4.7	6.8	5.3	4.1	3.5	15.3	13.9
Regen 2	4.6	4.4	5.4	4.7	4.6	4.0	7.1	6.3

Area Summary (number of pixels)		
	Frame 2b	Frame 2c
Mine floor	5185	5168
Regeneration 1	1576	1491
Native vegetation	6511	6370
Regeneration 2	1410	1380

Note that whereas the 2b and 2c means differ markedly before correction (Table 2), they agree closely after the correction procedure has been applied (Table 3). The values in the overlapping areas in the raw data were band-dependant and also varied with the nature of the materials. Differences were in the order of 15-30% between the bright and dark sides of the images. The correction produced coherence in the overlapping areas of better that 1% within a very low standard deviation.

The reflectance of a range of invariant targets (compared with a $BaSO_4$ Lambertian standard) using an Exotech field radiometer (Table 1) were made during the acquisition of the DMSV images. The mosaicked images were converted into reflectance values to provide a comparable measure of the vegetation status and the ability to compare between the two minesites over time.

Classification into vegetation associations was done on the mosaicked images with reference to field data. Fourteen different vegetation classes were established across the Andoom minesite. Statistics derived from these classes were then transferred to the adjacent Weipa minesite mosaic. Despite the 50% cloud cover, several days difference in acquisition and differences in camera settings, the cloud-free areas of the Weipa mosaic were satisfactorily classified using those classes.

Conclusion

A heuristic approach has been adopted for correcting shading effects across DMSV images that involves correlation with a near-simultaneously acquired Landsat TM image. With this method 196 differently illuminated DMSV images, collected in 1994, have been mosaicked and classified. Research is continuing to further refine the technique and to evaluate the effects of different solar angles and problems associated with the non-availability of near-simultaneously acquired TM data.

Some breakdown of this method was detected at boundaries of areas with large brightness differences (e.g. between bare mine floors and native vegetation), where a slight blurring trend can be observed near the edges because of the large difference in the spatial resolutions of the two datasets. A method for reducing this effect is being analysed. However, the results are satisfactory for the intended use in minesite rehabilitation monitoring.

References:

King, D. (1991) Determination and reduction of cover type differential illuminations with view angle in airborne multispectral video imagery. *Photogrammetric Engineering and Remote Sensing* 57:1571-1577.

Pickup,G., Chewings, V.H. and Pearce, G. (1995) Procedures for correcting high resolution airborne video imagery. *International Journal of Remote Sensing*. Vol 16, No. 9, 1647-1662

Lyon, R.J.P., Honey, F.R. and Hick, P.T. Second Generation Airborne Digital Multispectral Video: Evaluation of a DMSV for Environmental and Vegetation Assessment. *Proceedings of the First International Airborne Remote Sensing Conference and Exhibition*. Vol 2, 105-116